Klebsiella pneumoniae Nitrogenase: Formation and Stability of Putative Beryllium Fluoride−ADP Transition State Complexes†

Thomas A. Clarke, Faridoon K. Yousafzai, and Robert R. Eady*

Nitrogen Fixation Laboratory, John Innes Centre, Colney, Norwich NR4 7UH, U.K.

Received February 23, 1999; Revised Manuscript Received May 17, 1999

ABSTRACT: Incubation of the MoFe protein (Kp1) and Fe protein (Kp2), the component proteins of *Klebsiella pneumoniae* nitrogenase, with BeF_3^- and MgADP resulted in a progressive inhibition of nitrogenase activity. We have shown that at high Kp2 to Kp1 molar ratios this inhibition is due to the formation of an inactive complex with a stoichiometry corresponding to Kp1·{Kp2·$(MgADP·BeF_x)_2$}$_2$. At lower Kp2:Kp1 ratios, an equilibrium between this 2:1 complex, the partially active 1:1 Kp1·Kp2·$(MgADP·BeF_x)_2$ complex, and active nitrogenase components was demonstrated. The inhibition was reversible since incubation of the 1:1 complex in the absence of MgADP and beryllium resulted in complete restoration of activity over 30 h. Under pseudo-first-order conditions with regard to nitrogenase components and MgADP, the kinetics of the rate of inhibition with increasing concentrations of BeF_3^- showed a square dependence on [BeF_3^-], consistent with the binding of two Be atoms by Kp2 in the complex. Analytical fplc gel filtration profiles of Kp1·Kp2 incubation mixtures at equilibrium resolved the 2:1 complex and the 1:1 complex from free Kp1. Deconvolution of the equilibrium profiles gave concentrations of the components allowing constants for their formation of 2.1×10^6 and 5.6×10^5 M^{-1} to be calculated for the 1:1 and 2:1 complexes, respectively. When the active site concentration of the different species was taken into account, values for the two constants were the same, indicating the two binding sites for Kp2 are the same for Kp1 with one or both sites unoccupied. The value for K_1 we obtain from this study is comparable with the value derived from pre-steady-state studies of nitrogenase. Analysis of the elution profile obtained on gel filtration of a 1:1 ratio incubation mixture containing 20 μM nitrogenase components showed 97% of the Kp2 present initially to be complexed. These data provide the first unequivocal demonstration that Fe protein preparations which may contain up to 50% of a species of Fe protein defective in electron transfer is nevertheless fully competent in complex formation with MoFe protein.

Biological nitrogen fixation is catalyzed by nitrogenase, a two-component metalloenzyme system which couples the hydrolysis of MgATP to the reduction of dinitrogen in the reaction:

$$N_2 + 8H^+ + 8e + 16MgATP \rightarrow 2NH_3 + H_2 + 16MgADP + 16P_i$$

Mo-containing nitrogenases are made up of a molybdenum- and iron-containing protein (MoFe protein) and an Fe protein which functions as a specific MgATP-dependent electron donor to the MoFe protein (see refs *1*−*3*). The X-ray crystal structures of both individual proteins and the putative ADP−AlF_4 transition state complex of the two proteins of *Azotobacter vinelandii* have been determined (see refs *1*, *4*−*6*). These studies have revealed that the MoFe protein has an $\alpha_2\beta_2$subunit structure in which each dimeric $\alpha\beta$ subunit pair binds a P cluster (a unique Fe_8-S_7 cluster) positioned at the subunit interface and an FeMo-cofactor center (Fe_7S_9Mo-homocitrate) within the α subunit (*4*). The consensus view is that the FeMoco center is the site of substrate binding and activation and that the P clusters function in electron transfer to the catalytic center from the Fe protein (see refs *2*, *4*, *5*). The Fe protein is a γ_2 dimer which has a single [4Fe4S] center ligated at the subunit interface and two nucleotide binding sites, one on each subunit (*6*, *7*). The binding of MgADP or MgATP to the isolated Fe protein results in conformational changes of the protein, an altered reactivity and spectroscopic properties of the Fe/S cluster, which have been well documented (see ref *2*).

The crystal structures of Av2[1] (*6*) and Cp2 (*7*) display a peptide folding pattern similar to other nucleotide binding proteins such as the G family of proteins and myosin where transient protein complexes couple nucleotide hydrolysis to signal and energy transduction processes (*1*, *6*, *7*). MgATP hydrolysis by nitrogenase requires the presence of both the Fe protein and the MoFe protein, and recently several groups

† Financial support for this work was provided by the Biotechnology and Biological Sciences Research Council as part of the Competitive Strategic Grant to the John Innes Centre and a research studentship to T.A.C.

* Address correspondence to this author at the Nitrogen Fixation Laboratory, John Innes Centre, Colney, Norwich NR4 7UH, U.K. Email: robert.eady@bbsrc.ac.uk. Telephone: 44 1603 456900, ext 2728. Fax: - 44 1603 454970.

[1] Abbreviations: The nitrogenase metalloproteins are abbreviated according to the genus and species of the diazotrophs from which they were isolated; e.g., the Fe protein from *Klebsiella pneumoniae* is Kp2, the *Azotobacter vinelandii* Fe protein is Av2, and the *Clostridium pasteurianum* protein Cp2; the MoFe protein is from *K. pneumoniae* is Kp1 etc.

10.1021/bi9904353 CCC: $18.00
Published on Web 07/14/1999

have exploited these similarities to form stable but inactive nitrogenase complexes of *A. vinelandii* (*8, 9*) and *K. pneumoniae* (*10, 11*) using AlF_4^- and MgATP or MgADP. Aluminum fluoride has been extensively used as a tool to examine MgATP binding by gated proteins; its primary role is that of a phosphate analogue (*12*−*14*). The crystal structure of the ADP−AlF transition state complex of Av nitrogenase shows two MgADP molecules bound to the Fe protein in a *ras* binding mode, approximately parallel to the subunit interface, and the spatial arrangement of the subunits of the Fe protein is altered, resulting in a more compact structure when compared with the isolated protein (*5*). The redox center of the Fe protein is also repositioned by binding, and the redox potential decreases to ∼−600 mV, thereby facilitating electron transfer, presumably to a P cluster (*15*). The parallels with myosin (*12*) and G proteins (*12, 13*) have led to the proposal that the ADP−AlF complex can be considered to be an analogue of the E−ADP·P_i species in which AlF_4 mimics the trigonal bipyrimidal geometry of the terminal phosphate undergoing nucleophilic attack by a water molecule. Small-angle X-ray scattering studies have shown that *K. pneumoniae* nitrogenase components form a similar complex in the presence of AlF_4^- and MgADP, and that Kp2 has undergone a conformational change (*10*). We have previously studied the kinetics of the rate of formation of the ADP−AlF_4 complex by Kp nitrogenase components and shown that partial occupancy of the P clusters and FeMoco center binding sites of Kp1 results in a conformational change in the protein which alters the rate of reaction with Kp2 to form the inhibited complex (*11*).

In the present paper, MgADP and beryllium fluoride (BeF_3^-) are used as an alternative to AlF_4^-as a phosphate analogue, to form complexes corresponding to stable E−ATP species of the nitrogenase complex. The use of beryllium fluoride to complex nitrogenase has not been reported previously. We describe here the isolation and characterization of an ADP−BeF_x complex of Kp nitrogenase, and present data consistent with the formation of an inactive 1:2 complex of Kp1·{Kp2(ADP·BeF_x)$_2$}$_2$ and a partially active 1:1 complex of Kp1·(Kp2(ADP·BeF_x)$_2$. In the absence of MgADP and BeF_3^-, activity is regained as Kp2 dissociates from the complex. Evidence is presented for a 4-fold difference in the values for the apparent equilibrium constants for the formation of the 1:1 and 1:2 complexes. However, when the active site concentrations are taken into consideration, the values are the same, consistent with the Kp2 binding sites on Kp1 being equivalent in the complex with no evidence for cooperativity. We also present data that Kp2 preparations are fully competent in complex formation with Kp1.

EXPERIMENTAL PROCEDURES

Chemicals. $BeCl_2$ was purchased from Aldrich, $MgCl_2$ from Fisons, sodium dithionite from BDH Merck, KF and K-ADP from Sigma. To prepare a 50 mM solution of BeF_3^-, equal volumes of 100 mM $BeCl_2$ and 500 mM KF were mixed.

Nitrogenase Preparation. The nitrogenase proteins Kp1 and Kp2 were purified from *K. pneumoniae* as described previously (*16, 17*). The specific activities of Kp1 and Kp2 as determined by acetylene reduction were 2100 and 1700 nmol min^{-1} mg^{-1}, respectively. The molybdenum content of the Kp1 protein was 1.9 Mo atoms/molecule, determined using inductively coupled plasma emission analysis after acid hydrolysis by Southern Analytical Ltd. (Brighton BN1 9PY, U.K.).

Complex Formation. The complex was formed by the anaerobic incubation of Kp1 with Kp2 at molar ratios ranging from 1:1 to 1:9 in an incubation mixture containing 50 mM HEPES buffer, pH 7.4, 20 mM sodium dithionite, 2 mM KADP, 5 mM $MgCl_2$, and approximately 2 mM BeF_3^-. At intervals, samples were removed for measurement of nitrogenase activity. In a typical experiment, ADP, $MgCl_2$, BeF_3^-, HEPES, and H_2O were added to a stoppered vial. Argon was bubbled through for 10 min before addition of dithionite. Kp1 and Kp2 were finally added to make a total volume of 1 mL. The method is a modification of that described for the formation of the MgADP−AlF_4−nitrogenase complex of Kp and Av nitrogenases (*9, 10*).

The kinetics of formation of the inhibited complex were measured from the progressive loss of activity of Kp1 when assayed in the standard nitrogenase assay system in the presence of excess Kp2. Acetylene reduction assays were performed according to published procedures (*17*). A 20 μL aliquot of incubated mixture was added to each assay, and additional Kp2 was added to bring the final molar ratio of Kp1 to Kp2 to 1:12. Specific activities were calculated in units of nanomoles of acetylene reduced per minute per milligram of Kp1 protein.

Metal Analysis. The beryllium content was determined on a sample of the complex from which excess Kp2 and BeF_3^- had been removed by gel filtration. The complex was formed in an incubation mixture containing Kp1 and Kp2 at a 1:9 molar ratio. After overnight incubation, the mixture was purified by anaerobic passage through a Superdex S200 gel filtration column (Hiload 26/60) using the fplc system. The column was equilibrated with HEPES buffer, pH 7.4, containing 2 mM dithionite, to remove excess beryllium fluoride and excess Kp2. The recovered protein complex from the leading edge of the elution profile (1.24 mg) was wet-ashed using sulfuric acid and hydrogen peroxide and analyzed for Be using inductively coupled plasma emission analysis by Southern Analytical Ltd. Protein concentration was determined by the microbiuret method.

Isolation of Complexes by Gel Filtration. Complexes were prepared and purified by gel filtration of the incubation mixtures, using either a preparative Hiload 26/60 Superdex 200 column or an analytical HR 10/30 Superdex 200 column equilibrated with 50 mM HEPES, pH 7.4, containing 2 mM dithionite and 2 mM BeF_3^-. In some experiments as indicated, BeF_3^- was omitted from the buffer. When the elution profiles of the complexes were analyzed quantitatively, the absorbance was corrected for the minor contribution made by oxidized Kp2 using relative extinction coefficients of 1, 1.18, and 1.36 for Kp1, the Kp1Kp2$_{ox}$ complex, and the Kp1(Kp2$_{ox}$)$_2$ complex, respectively (*17, 18*).

ADP Analysis. The complex was prepared and purified by gel filtration as described above. ADP was extracted from the isolated complex (0.3 mg of protein) by the addition of an equal volume of $HClO_4$ to give a final concentration of 3.5% (v/v). Solid $KHCO_3$ was then added to neutralize the acid, and samples were centrifuged at 13 Krpm for 1 min to remove denatured protein. Aliquots (20 or 40 μL) of the

supernatant containing ADP were removed and analyzed by HPLC on a Waters 626 LC, and 996 photodiode array detector. The column used was a Symmetry Shield HPLC column (100 Å pore size, 5 μm particle size; Waters Ltd., Watford, U.K.), equilibrated with phosphate buffer, pH 6.8, flowing at a rate of 0.4 mL/min. Data were analyzed using a Millennium data acquisition package; integration of the ADP peak area allowed quantification of ADP concentration by comparison with standards subjected to the precipitation procedure used in the preparation of samples.

RESULTS AND DISCUSSION

X-ray crystallographic (*5*) and small-angle X-ray scattering studies (*10*) of stable nitrogenase complexes have previously been made in attempts to define the structure of potential protein intermediates formed during the catalytic cycle of the enzyme. Such protein complexes of Av (*5*, *8*, *9*, *15*) and Kp nitrogenase components (*10*, *11*), with bound ADP and AlF_4^-, have been characterized. By analogy with other systems, in these complexes the AlF_4^- behaves as a phosphate analogue and is hexacoordinate, and the nucleotide−AlF_4^- complex is held in a long-lived bound state corresponding to a transition state approaching nucleotide hydrolysis (see ref *5*). To extend these studies, we have tested the potential for beryllium fluoride−ADP to form tight complexes with nitrogenase. In such complexes, the BeF_3^- would be expected to be tetrahedrally coordinated and mimic a transition state of nitrogenase Fe protein in the ATP-bound conformation. A comparison of the structures and properties of these potential alternative conformations may give insight to the role(s) of nucleotides and Fe protein in nitrogenase function, as has been obtained from comparative X-ray structures of myosin where domain movements are seen only in the nucleotide−AlF_4^- complex (*14*).

Formation of a BeF_x−ADP Nitrogenase Complex. We adopted the strategy used to form the AlF−nitrogenase complex to test for the ability to form inhibited BeF complexes of nitrogenase. When Kp1 and Kp2 were preincubated under anaerobic conditions with BeF_3^- and MgADP before being assayed, a progressive loss of nitrogenase activity was observed (Figure 1a). This behavior would be expected if a long-lived transition state of nitrogenase−ADP−BeF_x was formed, as occurs on incubation with MgADP and AlF_4^- (*8*−*11*). The rate of formation of this putative transition state complex was monitored by measuring the residual activity of uncomplexed Kp1 species present in the reaction mixture when assayed in a standard nitrogenase assay system containing MgATP and additional Kp2. The progress of the inhibition (reaction 1) proceeded to equilibrium rather than completion, as indicated by experiments in which Kp1 and Kp2 were initially preincubated at a 1:1 molar ratio until activity measurements showed no further decrease in activity, at which time more Kp2 was added to increase the component ratio. Initially, a 15% inhibition was observed (Figure 1a), and when the Kp1:Kp2 ratio in the preincubation mixture was increased to 1:2, a further 15% inhibition was observed (Figure 1b). When, in the same preincubation mixture, the ratio was increased to 1:5, a very rapid inhibition of more than 95% was observed (Figure 1c). This behavior is consistent both with a system in dynamic equilibrium between the complex and its components and with Kp2 being only partially active in complex formation.

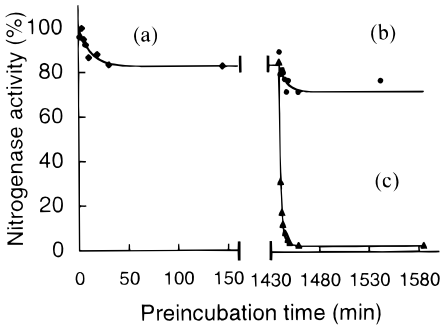

FIGURE 1: Effect on nitrogenase activity of the addition of Kp2 to a preincubation mixture of Kp2:Kp1 at a 1:1 molar ratio at equilibrium in the presence of BeF_3 and KADP. Nitrogenase components Kp2 and Kp1 (both 5.4 μM) were incubated in a mixture containing 50 mM HEPES buffer, pH 7.4; sodium dithionite, 20 mM; KADP, 2 mM; $MgCl_2$, 5 mM; and BeF_3^-, ~2 mM. At intervals, samples were removed for measurement of nitrogenase activity (resulting in a 50-fold dilution from the incubation conditions) as described under Experimental Procedures. After activity measurements indicated that equilibrium had been achieved (a), additional Kp2 was added to give a final 1:2 molar ratio (b) or a 1:5 molar ratio (c), and the subsequent effect on nitrogenase activity was determined.

It has been shown in pre-steady-state kinetic studies that preparations of Kp2 and Av2 are only ~50% functional in electron transfer (*19*, *20*). In the present case, it could be proposed that any inactive Kp2 present in our incubations may not form a complex with Kp1. Although Kp2 with a specific activity of 1700 (as used in our experiments) may not be fully active, in our kinetic analyses and the derivation of the association constants presented below, we have assumed that all Kp2 is competent in complex formation. Our reasoning is as follows: the data shown in Figure 4 below show no peak corresponding to free Kp2 on gel filtration of a 2:1 Kp2/Kp1 *incubation* mixture; such a peak is readily detectable at a 5:1 ratio. In addition, analysis of the elution profile of a 1:1 ratio incubation mixture containing 20 μM nitrogenase components from a gel filtration column (Figure 6) showed ~97% of the Kp2 present initially to be complexed. Neither of these observations is consistent with half the Kp2 preparation being unable to form a complex with Kp1, making our assumption that the data of Figure 1 reflect an equilibrium between nitrogenase components reasonable. These data provide the first unequivocal demonstration that Fe protein defective in electron transfer can complex with MoFe protein as is implicit in the Lowe−Thorneley scheme for nitrogenase function (see ref *2*).

The apparent association constants we derive below can be used to calculate the expected degree of inhibition under the conditions of Figure 1 as the amount of Kp2 is increased. The incubation mixture was diluted 50-fold in order to assay the residual Kp1 activity in the presence of excess Kp2. Under these diluted conditions, calculation using our determined value for the association constant of 2.1×10^6 M^{-1} predicts 14%, 25%, and 47% inhibition compared with the experimental values from Figure 1 of 15%, 30%, and 98%. These values are in good agreement for the first two values, but the last value observed is significantly higher than that calculated. We attribute this difference to the slow reestablishment of thermodynamic equilibrium in shifting from a 98% inhibition in the concentrated *incubation* mixture (5.4 μM Kp1 and 27 μM Kp2) (Figure 4) to the diluted assay

conditions (0.108 μM Kp1 and 0.54 μM Kp2). The additional Kp2, which is in 10-fold excess in the assay to optimize the measurement of Kp1 activity, is not considered in these calculations since BeF_3^- is diluted to a low level where inhibition would not be evident over the assay period. Consistent with this, the time course of substrate reduction during the assay of the partially inhibited complex was essentially linear for 30 min, indicating that dissociation was not occurring in the assay in the presence of MgATP.

Both proteins were required in the incubation mixture to form the inhibited complex since when MgADP and BeF_3^- (both 2 mM) were incubated with Kp1 or Kp2 separately, no detectable decrease in the activity of the incubated protein was observed over a 60 min period. This requirement for both components to be present is similar to that reported for the formation of the AlF_4−ADP complex of Fe protein and MoFe protein (*8, 9*). On the basis of the X-ray structure of the Av complex (*5*) and the well-documented interactions of nucleotides with Fe proteins (*2*), it is reasonable to assign $Kp2(MgADP)_2$ as the species *within the complex* which binds BeF_3^- as in eq 1

$$\text{Kp1} + 2\text{Kp2(MgADP)}_2 + n\text{BeF}_3^- \rightleftharpoons \text{Kp1}\{(\text{Kp2}\cdot\text{MgADP}_2)_2(\text{BeF}_x)\}_n \quad (1)$$

Isolation and Composition of the Beryllium Fluoride Complex. To investigate the stoichioimetry of the inactive complex, Kp1 was incubated overnight with a 10-fold excess of Kp2 in the presence of MgADP and BeF_3^-, and the complex was then separated from the excess Kp2 by gel filtration. When this incubation mixture was passed through an analytical Superdex 200 HR 10/30 column equilibrated with buffer containing BeF_3^- (50 mM) and sodium dithionite (0.2 mM), two symmetrical peaks were resolved within 15 min at a flow rate of 1.2 mL/min. Comparison with isolated Kp1 and Kp2 standards showed the later eluting peak coeluted with Kp2, while the earlier of the two peaks corresponded to a species with a molecular mass of 360 kDa. This elution pattern, together with the Be and ADP content indicated below, is consistent with a complex made up of one Kp1 and two Kp2 molecules being formed under these conditions.

To determine the beryllium and nucleotide composition of the complex, a scaled-up incubation mixture containing a Kp2:Kp1 ratio of 5:1 was purified by preparative gel filtration in the absence of MgADP and BeF_3^-. On the larger preparative column, the complex eluted after 99 min, followed by the excess Kp2 present in the incubation mixture at 133 min. Under these conditions, where the isolation of the complex took longer, the absorption peak corresponding to the complex was slightly asymmetric. The tailing edge was broader than the leading edge, indicating some dissociation was taking place during gel filtration in the absence of ADP or BeF_3^-, consistent with our kinetic analysis presented below. Material for analysis was taken from the leading edge.

The beryllium content determined for 1.24 mg of the complex was 13.3 nmol of Be, giving 3.83 Be atoms per molecule for a $Kp1\cdot(Kp2)_2$ complex. ADP analysis of a sample of this complex gave a value of 3.2 ± 0.2 ADP/(2Kp2/Kp1), indicating that the 2 nucleotide binding sites of Kp2 are only partially occupied. Previous studies with aluminum fluoride complexes of Av nitrogenase gave similarly low values for the ADP content, and it was proposed that it is not necessary for both ADP binding sites on the Fe protein to be occupied to enable complex formation (*8, 9*).

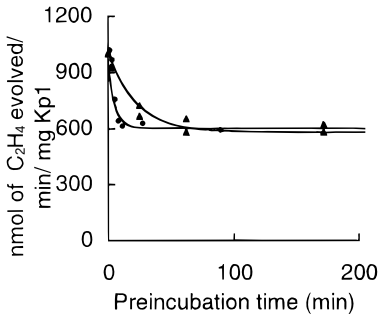

FIGURE 2: Effect of BeF_3 concentration on the rate of complex formation. In these experiments, Kp2:Kp1 was kept constant at a 2:1 molar ratio (Kp2 11.1 μM) while the [BeF_3^-] was (▲) 0.15 mM or (●) 0.35 mM. Other conditions are as described in the legend to Figure 1. The lines are a fit to eq 2.

Complex Formation Has a Square Dependence upon Concentration of BeF_3. Initial experiments showed that the rate of reaction was dependent not only on the concentration of nitrogenase components but also on the BeF_3^- concentration. By keeping Kp1 and Kp2 concentrations constant and varying the concentration of BeF_3^-, the relationship between BeF_3^- and Kp2 was explored. The rate of binding of MgADP to $Kp2_{ox}$ has been determined from stopped-flow spectroscopy and shown to be very rapid with a rate of 6×10^6 $M^{-1}\cdot s^{-1}$ (*19*). To determine whether Kp2·ADP reacts to form a complex with Kp1 which subsequently binds BeF_3^- to generate the inhibited complex, or if $Kp2(MgADP)_2BeF_3^-$ reacts with Kp1, a series of reactions were conducted at saturating [MgADP]. In these experiments, Kp2:Kp1 was kept constant at 2:1 molar ratio while [BeF_3^-] was varied from 0.1 to 0.35 mM. Pseudo-first-order conditions were maintained by keeping [BeF_3^-] ≫ [Kp2] or [Kp1]. Typical plots of the remaining activity, which represent the molar concentration of the catalytically active sites, [Kp1]*, of Kp1 that are left unreacted at any time *t*, are shown in Figure 2. Values of [Kp1]* were calculated as described previously (*11*). The solid points of these plots are the experimental points while the lines drawn through these points are the theoretical values generated by eq 2, and show a good fit to the data:

$$a = a_0 \exp^{k_{obs}\cdot t} - a_e \quad (2)$$

where a = residual activity, a_0 = initial activity, k_{obs} = a pseudo-first-order rate constant, t = time in seconds, and a_e = activity at equilibrium.

A plot of k_{obs} against the square of [BeF_3^-] gave a linear line with a positive intercept on the *y*-axis (Figure 3), and thus eq 3 is applicable, consistent with the rate-limiting step of complex formation involving two molecules of BeF_3^-, and the positive intercept indicates the reaction is reversible.

$$k_{obs} = k_1[\text{BeF}_3^-]^2 + k_2 \quad (3)$$

The dependence of k_{obs} on the square of [BeF_3^-] provides the first kinetic evidence for the binding of two BeF_3^- to Kp2 in the rate-limiting reaction for complex formation.

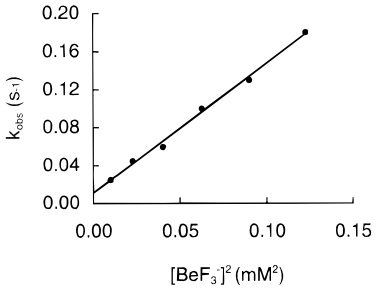

FIGURE 3: Dependence of the rate of complex formation (k_{obs}) on [BeF_3]. The [BeF_3^-] was varied from 0.1 to 0.35 mM as indicated, and k_{obs} for the rate of loss of nitrogenase activity was determined from a fit to eq 2. Note the square dependence of k_{obs} on [BeF_3].

These kinetic analyses potentially provide information on the order of assembly of the inhibited complex. We consider two possibilities: first, the mechanism shown below (eq 4), in which the rate-limiting step in the formation of the inhibited complex is the reaction between BeF_3^- and Kp2-$(MgADP)_2$, followed by binding of Kp2$(MgADP{\cdot}BeF_3^-)_2$ to vacant sites on Kp1:

$$Kp2{\cdot}(MgADP)_2 + 2BeF_3^- \rightleftharpoons Kp2(MgADP{\cdot}BeF_3^-)_2 \quad (4)$$

The binding of MgADP to reduced Kp2 is generally assumed to be very rapid, as has been reported for the binding of MgADP to $Kp2_{ox}$ where a value of 6×10^6 $M^{-1}{\cdot}s^{-1}$ was obtained (*16*); a slow exchange of MgADP from Kp2 has been reported (*20*), but it had no effect on activity. However, when MgADP and BeF_3^- were incubated together with the Kp2 alone, no loss of activity was observed even after 60 min incubation. This makes any reaction involving isolated Kp2, or any slowly dissociating species with an altered conformation caused by MgADP−BeF_3^- binding to the protein, an unlikely candidate for the reversible rate-limiting step for complex formation.

An alternative mechanism is one in which Kp1 and Kp2 react initially to form Kp1·Kp2$(MgADP)_2$ complex followed by reaction of BeF_3^- to yield the catalytically inactive transition-state complex:

$$Kp1{\cdot}Kp2(MgADP)_2 + 2BeF_3^- \rightleftharpoons Kp1{\cdot}Kp2(MgADP{\cdot}BeF_3^-)_2 \quad (5)$$

In this case, the reaction involving BeF_x (eq 5) would be the rate-limiting step. Since the results show a square dependence on [BeF_3^-], a full occupancy of Kp2 nucleotide binding sites appears to be required for formation of the inhibited complex. This proposal is similar to that of Renner and Howard for the AlF−ADP complex of Av nitrogenase (*8*), who suggested that the most probable site of interaction of AlF_4^- was with the two-component complex in which the Fe protein was in the nucleotide-bound conformation.

Gel Filtration Behavior of Incubation Mixtures Containing Increasing Kp2:Kp1 Ratios. The kinetic studies presented above indicate that the Kp1·{Kp2$(MgADP.BeF_x)_2\}_2$ complex is in slow equilibrium with BeF_3^- and Kp1·Kp2$(MgADP)_2$. To gain some insight into the stability and composition of the potential complexes formed, we investigated their behavior on analytical gel filtration. Incubation mixtures containing Kp2:Kp1 at molar ratios of 1:1, 2:1, and 5:1 were prepared as described under Experimental Procedures, and subjected to gel filtration using an analytical Superdex S-200 HR 10/30 column. In such mixtures, species corresponding to protein complexes in order of decreasing molecular weight, i.e., Kp1$(Kp2)_2$, Kp1(Kp2), Kp1, and Kp2, can be expected to be present in varying amounts. At 5:1, the highest ratio examined, where activity measurements indicated that complex formation was essentially complete (Figure 1c), the elution profile (at a flow rate of 0.8 mL/min) showed a leading peak eluting at 9.25 mL (compared with 10.66 mL for free Kp1), followed by a second peak at 12.27 mL associated with free Kp2 (Figure 4). The peak profile of the leading species was slightly asymmetric on the trailing edge. Since this was not observed in the profile of Kp1 alone, it is unlikely to be a result of matrix/protein interaction which is probably indicative of migration of a mixture of species, dominated by a component larger than Kp1. As the ratio of Kp2:Kp1 in the incubation mixture was decreased to 2:1, the elution profile broadened, and the retention volume of the peak became greater. Finally, at the 1:1 molar ratio, it was partially resolved into two peaks (Figure 4). This behavior is consistent with a decreasing contribution of higher molecular weight species to the absorbance profile as the Kp2:Kp1 ratio of the proteins in the incubation mixture is lowered.

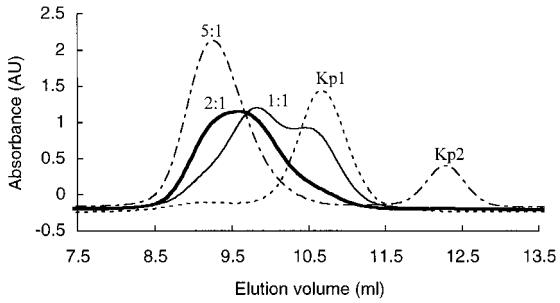

FIGURE 4: Analytical gel filtration profiles of Kp1 and preincubation mixtures containing different Kp2:Kp1 molar ratios. Preincubation mixtures, as described in the legend to Figure 1, were prepared with different ratios of Kp1 and Kp2 as indicated. After 18 h incubation, they were passed through an analytical Superdex 200 HR 10/30 column equilibrated with 50 mM HEPES buffer, pH 7.4, containing BeF_3^- (2 mM) and sodium dithionite (0.2 mM). The flow rate was 0.8 mL/min, and the absorbance of the eluted material was monitored at 410 nm.

During zone transport (as in our gel filtration experiments) of interacting systems in slow equilibrium, the extent to which component species can be resolved is dependent on the transit time of the material undergoing chromatography, relative to the rate of dissociation. To investigate the stability of the complexes during gel filtration, the effect of flow rate on the elution profile of incubation mixtures containing Kp2:Kp1 at a molar ratio of 5:1 was examined. The elution profile of the leading peak of the mixture maintained a constant area and eluted in this series of experiments at 9.4 ± 0.05 mL over a range of flow rates from 1.2 to 0.2 mL/min (data not presented). The independence of the retention volume on flow rate indicates that the components are not in rapid equilibrium under these conditions, and that the elution peak is dominated by a discreet Kp1$(Kp2)_2$ complex of M_r ~360 000. The stability of this form of the BeF complex of Kp nitrogenase on gel filtration is comparable to that reported for the AlF complex of Av nitrogenase (*8*, *9*).

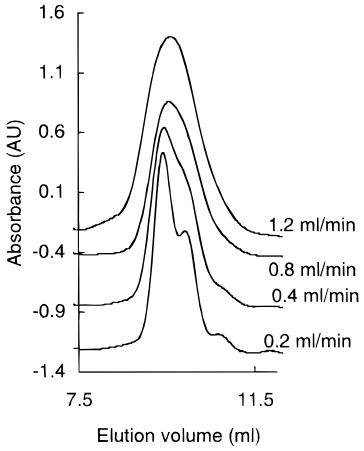

FIGURE 5: Effect of flow rate on elution profiles of a 2:1 incubation mixture. A preincubation mixture of a 1:2 molar ratio of Kp1 and Kp2 was prepared as described in the legend to Figure 1. After 18 h incubation, samples were analyzed as in Figure 2 except the flow rate was varied as indicated.

In contrast, elution profiles of the 2:1 incubation mixture showed a significant dependence on the flow rate (see Figure 5). As the flow rate decreased over the same range, the leading peak became sharper and the retention volume decreased from 9.52 to 9.42 mL. At the lowest flow rate, the retention volume of 9.42 mL for this leading peak was within the range of values obtained for the 1:2 complex present in a 5:1 incubation mixture as described above. However, as the flow rate was decreased, two slower components were partially resolved, one at 9.95 mL and a second at 10.7 mL corresponding to free Kp1.

Our interpretation of these data is that an incubation mixture of a 2:1 molar ratio of Kp2:Kp1 contains, at equilibrium, both the Kp1·Kp2 and Kp1$(Kp2)_2$ complexes in addition to free nitrogenase components, consistent with the retention of some activity by such mixtures (Figure 1). The peak at a retention volume of 9.95 mL, resolved at slow flow rates, corresponds to the 1:1 complex Kp1·Kp2. The dramatic effect of flow rate on resolution between 0.2 and 0.4 mL/min was unexpected. That this effect was due to increased resolution at low flow rates during gel filtration, rather than dissociation during chromatography, was established by the behavior of the isolated 1:1 complex during gel filtration. In this case, decreasing the flow rate to 0.15 mL/min resulted in resolution from free Kp1 which was not evident at 1 mL/min (data not shown).

Determination of the Apparent Equilibrium Constants for Complex Formation. Gel filtration of a 1:1 molar ratio incubation mixture at 0.2 mL/min showed an elution profile comprised of three partially resolved peaks. The leading peak eluting at 9.4 mL corresponded to the Kp1$(Kp2)_2$ complex discussed above, a second major peak eluting at 9.95 mL to a 1:1 Kp1Kp2 complex, and the third to uncomplexed Kp1 (10.7 mL). This profile is consistent with these species arising from a mixture formed by the two sequential reactions in which Kp2 binds successively to the two binding sites on Kp1:

$$\text{Kp1} + \text{Kp2(MgADP)}_2 \underset{\text{BeF}_3^-}{\overset{K_1}{\rightleftharpoons}} \text{Kp1·Kp2(MgADP)}_2 \quad (7)$$

$$\text{Kp2(MgADP)}_2 + \text{Kp1·Kp2(MgADP)}_2 \underset{\text{BeF}_3^-}{\overset{K_2}{\rightleftharpoons}} \text{Kp1·\{Kp2(MgADP)}_2\}_2 \quad (7)$$

In such a mixture, nitrogenase activity shows no further decrease after 50 min (Figure 1), indicating that the formation of the inhibited complexes has reached equilibrium after this time. Since the dissociation of the complexes does not occur during gel filtration in the presence of BeF_3^-, deconvolution of the fplc elution profiles of these mixtures allows the concentrations of species defined in eqs 6 and 7 to be determined, and the equilibrium constants K_1 and K_2 to be calculated. Incubation mixtures at equilibrium containing Kp1 and Kp2 at a 1:1 molar ratio in the concentration range 5−50 μM were subject to gel filtration. The profiles of 20 and 50 μM mixtures were the same, with the 1:1 complex predominating over the 2:1 complex and the excess of uncomplexed Kp1. However, as the concentration of nitrogenase components in the preincubation mixture was decreased further, the concentration of free Kp1 increased, consistent with dissociation of the complex occurring, but the amount of the 1:2 complex decreased more rapidly relative to the 1:1 complex which remained essentially constant as the concentration was decreased over this range (Table 1 and Figure 6). Analysis of these data gave average values for the apparent equilibrium constants of 2.07×10^6 M^{-1} for K_1 and 5.58×10^5 M^{-1} for K_2, respectively (Table 1). Since K_2 is about 4-fold smaller than K_1, it is apparent that the 1:1 complex Kp1·Kp2$(MgADP·BeF)_2$ is more stable than the 2:1 complex Kp1·\{Kp2$(MgADP·BeF)_2\}_2$, despite the two binding sites on Kp1 being equivalent. It might be argued that this difference in stability arises from cooperative behavior between the two sites involving long-range conformational changes in Kp1 following binding of a single Kp2. However, when [Kp1], [Kp1·Kp2$(MgADP·BeF)_2$], and [Kp1·\{Kp2$(MgADP·BeF)_2\}_2$] are corrected for their molar active site concentration available for the forward and reverse reactions, eqs 6 and 7 (i.e., [Kp1] and [Kp1·\{Kp2$(MgADP·BeF)_2\}_2$] are multiplied by 2), the new intrinsic equilibrium constants, $*K_1$ and $*K_2$, are equal. This indicates that the active site concentrations of Kp1, [Kp1·Kp2$(MgADP·BeF)_2$], and [Kp1·\{Kp2$(MgADP·BeF)_2\}_2$] available for their respective reactions at equilibrium are the same, and the binding of Kp2 to one site on Kp1 does not change the affinity of the other site. Thus, under our conditions, the two Kp2 binding sites on Kp1 function independently.

The value for K_1 we obtain, 2.07×10^6 M^{-1}, is very close to the value of 3.3×10^6 M^{-1} determined from a pre-steady-state kinetic analysis of stopped-flow studies of Lowe-Thorneley for the reactions of $Kp2_{ox}(MgADP)_2$·Kp1 (*21*). The similarity of these values suggests that the factors controlling complex formation in nitrogenase turnover and those involved in the formation of the inhibited transition state complex are the same. Thus, in the analyses above, it is a reasonable assumption that reduced Kp2 with MgADP bound is the reactive species in complex formation.

In the present study, no evidence for interactions between the two binding sites for Kp2 on Kp1was observed, although the statistical factor of the apparent equilibrium constants results in the 1:1 complex appearing to be a more stable species than the 2:1 complex. In contrast, the binding of mutated forms of Av2 to Av1, measured by their ability to

Table 1: Deconvolution of Analytical Gel Filtration Peak Profiles at Different Concentrations of 1:1 Kp1:Kp2 Molar Incubation Mixtures: Calculated Values for the Equilibrium Constants K_1 and K_2 for the Formation of 1:1 and 1:2 Complexes

concntration of 1:1 incubation mixture (μM)	height of 1:2 peak (%)[a]	height of 1:1 peak (%)[a]	height of Kp1 peak (%)[a]	K_1 (M^{-1})	K_2 (M^{-1})	ration of equilibrium constants
20	23.7	48.9	27.3	2.44×10^6	6.65×10^5	3.7
10	21.6	48.8	29.6	2.06×10^6	5.53×10^5	3.7
5	17.8	48.0	34.2	1.71×10^6	4.55×10^5	3.8
	average of equilibrium constants:			$(2.07 \times 10^6) \pm (0.36 \times 10^6)$	$(5.58 \times 10^5) \pm (1.05 \times 10^5)$	3.7

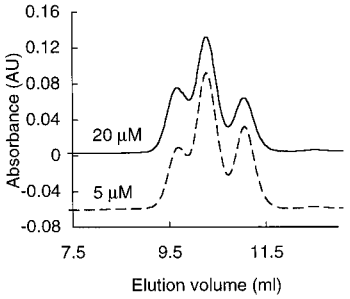

FIGURE 6: Effect of nitrogenase concentration on the composition of preincubation mixtures at equilibrium. Preincubation mixtures containing Kp2:Kp1 at a molar ratio of 1:1 were set up as described in the legend to Figure 1 except that the concentration of nitrogenase was 5 or 20 μM. After 18 h incubation, they were passed through an analytical fplc Superdex 200 HR 10/30 column equilibrated with 50 mM HEPES buffer, pH 7.4, containing BeF_3^- (2 mM) and sodium dithionite (0.2 mM). The flow rate was 0.15 mL/min, and the absorbance of the eluted material was monitored at 410 nm.

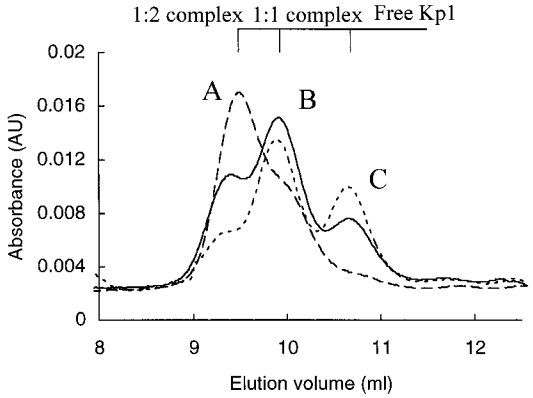

FIGURE 7: Time dependence of the elution profile of the 1:2 complex. Isolated 1:2 complex was prepared by preparative gel filtration and then, after incubation for different periods, passed through an analytical fplc Superdex 200 HR 10/30 column equilibrated with 50 mM HEPES buffer, pH 7.4, containing sodium dithionite (0.2 mM), but no BeF_3^-. (A) As isolated; (B) after 12 h; (C) after 36 h. The flow rate was 0.15 mL/min, and the absorbance of the eluted material was monitored at 410 nm.

inhibit activity of the wild-type enzyme, showed sigmoidal inhibition kinetics suggestive of cooperativity in the binding of Av2 to Av1 (*23*, *24*). Long-range interactions across the $\alpha\beta$ subunit pairs of MoFe protein effecting reactivity for complex formation have been detected for Kp1, but no evidence for interaction of the Fe protein binding sites was observed (*11*). Clearly interactions of this type could potentially result in cooperativity for binding of Fe protein to the two binding sites on MoFe protein. The differences between the work reported here, where the apparent equilibrium constants were determined directly from the concentrations of species in solution and that involving the mutated Fe protein species (*23*, *24*), may reflect subtle conformational changes which occur during catalysis, since in the latter case inhibition of enzyme turnover was measured.

Stability of the Complexes. The stability of the isolated 2:1 and 1:1 complexes was determined from the time-dependent increase in activity which occurs on incubation in 50 mM HEPES, pH 7.4, containing 2 mM dithionite but no BeF_3^- or MgADP. Immediately after isolation by gel filtration, the specific activity of the 1:1 complex was 1100 nmol of C_2H_2 reduced min^{-1} (mg of Kp1)$^{-1}$. Subsequent assay after incubation in an anaerobic chamber at 15 °C resulted in essentially full recovery to a specific activity of 1960 after 30 h. The 2:1 complex showed similar behavior, increasing from an initial specific activity of 112 to 945 after 30 h. In this case, complete recovery of activity is not attained, because equilibrium is shifted from a 2:1 to a 1:1 complex equilibrium, where the 1:1 complex is then retained by the free components of the resulting mixture. These slow rates of dissociation could well arise from a slow relaxation of the altered conformation of Kp2 within the complex as ADP or BeF_3 dissociates from the Fe protein. Evidence for an altered conformation of Kp2 in the complex is provided by a small-angle X-ray scattering study of the Kp1·{Kp2-$(MgADP{\cdot}BeF_x)_2\}_2$ complex which shows the molecular envelope to be very similar to that of the Kp- and Av-ADP·AlF_4 transition state complexes (Grossman, Hasnain, and Eady, unpublished work), where the nature of the conformational change undergone by the Fe protein in the latter complex has been determined in an X-ray crystallographic study (*5*).

The stability of both the 1:1 and 2:1 complexes was also investigated using gel filtration. A preparative column equilibrated with buffer lacking BeF_3^- and ADP was used to isolate the 2:1 complex in order to determine possible time-dependent changes in the composition. Following the formation of the complex and its isolation by preparative gel filtration and subsequent passage through an analytical column, the elution profile of the zero time sample indicated that some dissociation had occurred. The profile showed the sample to be predominantly the 2:1 complex but also contained some 1:1 complex and free Kp1 (Figure 7A). After 12 h, the elution profile showed a marked decrease in the amount of 2:1 complex and an increase in the amount of 1:1 complex and free Kp1 (Figure 7B). The relative change in the amounts of the two complexes in this time indicates that the 2:1 complex dissociates initially to form the 1:1 complex. After 36 h, the amount of the 2:1 complex had decreased further, that of the 1:1 complex remained unchanged, and the Kp1 amount had increased (Figure 7C). This indicates that the rate of formation of the 1:1 complex produced by dissociation of the 2:1 complex and its rate of dissociation to form free Kp1 are essentially the same.

ACKNOWLEDGMENT

We gratefully acknowledge Prof. Barry Smith, Dr. Richard Henderson, and our other colleagues in the NFL for constructive discussions on data analysis and comments on the manuscript. We also thank Dr. Mike Naldrett for help with nucleotide analyses.

REFERENCES

1. Howard, J. B., and Rees, D. C. (1996) *Chem. Rev. 96*, 2965−2982.
2. Burgess, B. K., and Lowe, D. J. (1996) *Chem. Rev. 96*, 2983−3011.
3. Peters, J. W., Fisher, K., and Dean, D. R.(1995) *Annu. Rev. Microbiol. 49*, 335−366.
4. Peters, J. W., Stowell, M. H. B., Soltis, S. M., Finnegan, M. G., Johnson, M. K., and Rees, D. C. (1997) *Biochemistry 36*, 1181−1187.
5. Schindelin, H., Kisker, C., Shlessman, J. L., Howard, J. B., and Rees, D. C. (1997) *Nature 387*, 370−376.
6. Georgiadis, M. M., Komiya, H., Chakabarti, P., Woo, D., Kornuc, J. J., and Rees, D. C. (1992) *Science 257*, 1653−1659.
7. Schlessman, J. L., Woo, D., Joshua-Tor, L., Howard, J. B., and Rees, D. C. (1998) *J. Mol. Biol. 280*, 669−685.
8. Renner, K. A., and Howard, J. B. (1996) *Biochemistry 35*, 5353−5358.
9. Duyvis, M. G., Wassink, H., and Haaker, H. (1996) *FEBS Lett. 380*, 233−236.
10. Grossman, J. G., Hasnain, S. S., Yousafzai, F. K., Smith, B. E., and Eady, R. R. (1997) *J. Mol. Biol. 266*, 642−648.
11. Yousafzai, F. K., and Eady, R. R. (1997) *Biochem. J. 326*, 635−640.
12. Coleman, D. E. (1994) *Science 257*, 1677−1682.
13. Sobdek, J., Lambright, D. G., Noel, J. P., Hamm, H. E., and Sigler, P. B. (1994) *Nature 372*, 276−279.
14. Fisher, A. J., Smith, C. A., Thoden, J. B., Smith, A., Sutoh, K., Holden, H. M., and Rayment, I. (1995) *Biochemistry 34*, 8960−8972.
15. Spee, J. H., Arendsen, A. F., Wassink, H., Marritt, S. J., Hagen, W. R., and Haaker, H. (1998) *FEBS Lett. 432*, 55−58.
16. Yousafzai, F. K., Buck, M., and Smith, B. E. (1996) *Biochem. J. 318*, 111−118.
17. Eady, R. R., Smith, B. E., Cook, K. A., and Postgate, J. R. (1972) *Biochem. J. 133*, 655−675.
18. Thorneley, R. N. F., and Lowe, D. J. (1983) *Biochem. J. 215*, 383−403.
19. Ashby, G. A., and Thorneley, R. N. F. (1987) *Biochem J. 246*, 455−465.
20. Lanzilotta, W. N., Fisher, K., and Seedfelt, L. C. (1996) *Biochemistry 35*, 7188−7196.
21. Miller, R. W., Eady, R. R., Gormal, C., Fairhurst, S. A., and Smith, B. E. (1998) *Biochem. J. 334*, 601−607.
22. Lowe, D. J., and Thorneley, R. N. F. (1984) *Biochem. J. 224*, 895−901.
23. Lanzilotta, W. N., Ryle, M. J., and Seedfelt, L. C. (1995) *Biochemistry 34*, 10713−10723.
24. Lanzilotta, W. N., Fisher, K., and Seedfelt, L. C. (1997) *J. Biol. Chem. 272*, 4157−4165.

BI9904353